JES

JOURNAL OF
ENVIRONMENTAL
SCIENCES

www.jesc.ac.cn

Removal of Ni(II) from strongly acidic wastewater by chelating precipitation and recovery of NiO from the precipitates

Xin Yang [1,2,3], *Xianjia Peng* [1,2,3,*], *Linghao Kong* [1,2], *Xingyun Hu* [1,2]

[1] State Key Laboratory of Environmental Aquatic Chemistry, Research Center for Eco-Environmental Sciences,
Chinese Academy of Sciences, Beijing 100085, China
[2] Beijing Key Laboratory of Industrial Wastewater Treatment and Resource Recovery, Research Center for
Eco-Environmental Sciences, Chinese Academy of Sciences, Beijing 100085, China
[3] University of Chinese Academy of Sciences, Beijing 100049, China

ARTICLE INFO

ABSTRACT

Strongly acidic wastewater produced in nonferrous metal smelting industries often contains high concentrations of Ni(II), which is a valuable metal. In this study, the precipitation of Ni(II) from strongly acidic wastewater using sodium dimethyldithiocarbamate (DDTC) as the precipitant was evaluated. The effects of various factors on precipitation were investigated, and the precipitation mechanism was also identified. Finally, the nickel in the precipitates was recovered following a pyrometallurgical method. The results show that, under optimised conditions (DDTC:Ni(II) molar ratio = 4:1; temperature = 25 °C), the Ni(II) removal efficiency reached 99.3% after 10 min. In strongly acidic wastewater, the dithiocarbamate group of DDTC can react with Ni(II) to form DDTC–Ni precipitates. Further recovery experiments revealed that high-purity NiO can be obtained by the calcination of DDTC–Ni precipitates, with the nickel recovery efficiency reaching 98.2%. The gas released during the calcination process was composed of NO_2, CS_2, H_2O, CO_2, and SO_2. These results provide a basis for an effective Ni(II) recovery method from strongly acidic wastewater.

Introduction

Nonferrous metal-smelting industries generally produce large amounts of strongly acidic wastewater that contains nickel, arsenic, copper, zinc, and iron, with high H_2SO_4 concentrations (5%–20%). For environmental and economic reasons, high-value heavy metals in this type of wastewater should be recovered. Owing to its strength and high temperature- and corrosion-resistance properties, nickel is considered as a strategic metal and is widely used in various industries, including chemical engineering, aerospace, and electronic communication (Orhan et al., 2002; Coman et al., 2013; Tao et al., 2016; Hussain et al., 2017). Additionally, in recent years, the price of nickel has risen sharply due to the increase in global demand, exceeding $16,000 per ton in China (Peng et al., 2014). Therefore, an effective method of recovering nickel from acidic wastewater should be developed.

Neutralisation is the most conventional method of removing heavy metal ions from strongly acidic wastewater.

However, this method not only wastes the heavy metal resources in strongly acidic wastewater, but also produces large amounts of hazardous waste. It will be interesting to selectively remove heavy metals under strongly acidic conditions and then recycle the wastewater, by which, heavy metals can be recycled and the production of hazardous waste can be avoided. Sulphide precipitation is the most widely adopted method of recovering metal ions from strongly acidic wastewater, in which, sulphides such as H_2S, Na_2S, and FeS, are utilised as precipitants (Kong et al., 2017; Zhang et al., 2020). This method is efficient in precipitating arsenic and copper. However, sulphides could not precipitate Ni(II) under strongly acidic conditions (pH < 2), because the principle sulfide species participating in the nickel sulfide precipitation reaction is bisulfide (HS^-), and sulphides is greatly limit in producing disulfide ions at pH < 3.5 (Karbanee et al., 2008; Lewis, 2010). Solvent extraction is effective for recovering nickel ions from acidic wastewater (Tanaka et al., 2008; Deep et al., 2010; Chen et al., 2015; Wei et al., 2016). However, this method is generally applied under weakly acidic conditions (pH 3.0 − 6.0), as high H^+ concentrations reduce the extraction efficiency and distribution ratio of nickel ions under strongly acidic conditions (pH < 2.0) (Sulaiman et al., 2018; Li et al., 2011). Therefore, an in-depth investigation of the recovery of Ni(II) that cannot be precipitated by sulphides must be conducted.

Many researchers and engineers have recently studied chelating precipitation to remove nickel ions from wastewater due to its simple operation, high efficiency, and potential for industrialisation (Fu et al., 2007) Chelating precipitation is a method of removing heavy metals by the formation of insoluble chelates using strong chelating agents (Matlock et al., 2002). According to the hard and soft acids and bases (HSAB) principle, Ni(II) is a Lewis acid. Therefore, it is reasonable to assume that Ni(II) can be removed from wastewater using soft bases with a sulphur-containing functional group (Pearson, 1968; Matlock et al., 2003). Organic sulphur-containing precipitants, such as sodium dimethyldithiocarbamate (DDTC), sodium trithiocarbonate (STC), and sodium trimercaptotriazine (TMT), are typically used to remove Ni(II) from wastewater. For example, previous studies have shown that DDTC can effectively remove Ni(II) under optimal conditions (DDTC:Ni(II) molar ratio = 2; pH = 7.0), achieving residual concentrations as low as 0.76 mg/L (Fu et al., 2007) STC is used to treat nickel-containing acidic wastewater generated from printed circuit board manufacturing. In one study, Ni(II) was effectively removed using a stoichiometric STC dosage at pH 9.0–9.5, and its concentrations could be reduced to < 0.009 mg/L (Thomas et al., 2018a). Similarly, as another organic sulfur-containing precipitant, TMT has also been used as a precipitant to remove Ni(II) from washing water produced in flue gas purification (Decostere et al., 2009). It was found that a low residual Ni(II) concentration of < 0.023 mg/L could be obtained under a stoichiometric TMT dosage after the acid-washing water (pH = 0.5) was neutralised to pH 6.0–7.0 using lime milk. The effective removal of Ni(II) by chelation has been achieved under weakly acidic, neutral, or weakly alkaline conditions, however, few studies were focused on the removal of Ni(II) under strongly acidic conditions. Additionally, the re-

moval of Ni(II) from strongly acidic wastewater by chelating precipitation has little been reported.

The main aim of this study was to develop an easily implemented selective recycling process with high recovery efficiency from nickel-containing acidic wastewater produced by nickel smelting. Therefore, the effective recovery of Ni(II) from strongly acidic wastewater using organic sulphur-containing chelating agents is investigated in this study. First, the Ni(II) removal efficiency of organic sulphur-containing chelating agents (DDTC, TMT, and STC) is examined. Second, the impacts of key variables on the Ni(II) removal efficiency are investigated, including the DDTC:Ni(II) molar ratio, H_2SO_4 concentration, reaction time, and temperature, and the Ni(II) removal mechanism is identified. Finally, the recovery of NiO from the precipitates using the pyrometallurgical method is studied, and the gas released by calcination identified.

1. Materials and methods

1.1. Reagents and materials

All reagents used in this study are described in the Supplementary Material. Deionised water was used to prepare all solutions in the experiments. DDTC and TMT stock solutions (50.0 g/L) were prepared by dissolving the required amounts of the reagents (DDTC or TMT) in deionised water; STC was used as a 40.0% solution as obtained without further treatment.Simulated strongly acidic wastewater was prepared by adding $NiSO_4•6H_2O$, $ZnSO_4•7H_2O$, or $FeSO_4•7H_2O$ to a H_2SO_4 solution at specified concentrations. Unless otherwise stated, the Ni(II) and H_2SO_4 concentrations in all simulated wastewaters were 100.0 mg/L and 1.02 M, respectively. Additionally, strongly acidic wastewater was sampled from a nickel smeltery in Gansu Province, China, which was pre-treated with Na_2S to remove Cu(II) and As(III) before the Ni(II) recovery experiments. The chemical composition of the nickel smeltery wastewater is shown in Appendix A **Table S1**.

1.2. Screening of organic sulphur-containing precipitants

The concentrations of H_2SO_4 and metal ions in the simulated wastewater are shown in Appendix A **Table S2**. Typically, a certain dose of precipitant was added to 400 mL of the simulated wastewater, which was then stirred (250 r/min) in a thermostatic magnetic stirring water bath (EMS-30, Changzhou Langyue Instrument Co., Ltd.) at 25 °C for 20 min. Next, 5-mL suspensions were collected and filtered through 0.22-µm PES membrane filters to determine the residual Ni(II) concentrations. Finally, the precipitates were separated using microporous membrane filters, repeatedly washed with deionised water, and dried before characterisation by X-ray diffraction (XRD) characterisation, elemental analysis, and Fourier transform-infrared spectroscopy (FT-IR).

1.3. Ni(II)-removal experiments

Ni(II)-removal experiments were conducted in 500-mL beakers with 400 mL of simulated wastewater and continuous stirring in a thermostatic magnetic stirring water bath. At certain time intervals, 5-mL samples of the suspension were collected and filtered through 0.22-µm PES membrane filters to determine the residual Ni(II) concentrations. In each case, after the reaction had completed, the precipitates were separated using 0.45-µm microporous membrane filters, then rinsed repeatedly using deionised water, and finally dried in a vacuum drying oven at 105 °C for further analysis.

1.4. Recovery of nickel oxide by calcination of DDTC–Ni

In each experiment, after completing precipitation, the precipitates were separated using a vacuum filter bottle and then repeatedly rinsed with deionised water, and dried for 6 hr at 70 °C in a vacuum drying oven to obtain a green powder. These samples were then calcined in a tubular vacuum furnace (Beijing Cinite Technology Co., Ltd., China) under a constant airflow. The temperature of the furnace increased from 25 to 900 °C at a rate of 10 °C/min. Finally, the samples were calcined at 900 °C for 1 hr to obtain NiO.

1.5. Analytical methods

To establish a standard curve for DDTC, 20 mg/L of DDTC was directly analysed by wavelength scanning using a UV–Vis spectrophotometer (DR6000, Hach, USA) in the range of 200–400 nm. As shown in Appendix A **Fig. S1**, DDTC exhibited two absorption maxima at 254 and 278 nm in the UV region. The bands at 254 and 278 nm were attributed to a $\pi \rightarrow \pi^*$ transition in the N–C–S group and an $n \rightarrow \pi^*$ transition in the S–C = S group, respectively (Vandebeek et al., 1970; Zhen et al., 2012). The S–C = S group is the main functional group that reacts with metal ions; therefore, the absorption values at 278 nm could indicate the DDTC concentration (Yan et al., 2019). The derived standard curve of the DDTC concentrations is shown in Appendix A **Fig. S2**.

The dimethylamine (DMA) concentration of the solutions was determined by ion chromatography (ICS-1100, Dionex, USA), the chromatographic conditions of which are described in Appendix A Supplementary data (Li et al., 2009). The standard curve for the DMA concentrations is shown in Appendix A **Fig. S3**. The concentration of CS_2 was measured following the diethylamine cupric acetate spectrophotometric method (Hunt et al., 1973), and the standard curve is displayed in Appendix A **Fig. S4**. The concentration of H_2S was determined following the methylene blue method (Silva et al., 2001), and the derived standard curve is shown in Appendix A **Fig. S5**.

The concentrations of Ni(II), Zn(II), and Fe(II) were analysed by inductively coupled plasma-optical emission spectrometry (ICP-OES) (NexION300, PerkinElmer, USA), and the crystallinity of the obtained powder was characterised by XRD (X'Pert Pro-MPD, PANalytical, Holland). The TMT and DDTC functional groups were analysed before and after the removal of Ni(II) using a Fourier transform-mid-infrared spectrometer (FT-MIR; Nicolet iS50, Thermo Fisher, USA) with a wavenumber range of 500–4000 cm^{-1}. The far-infrared spectra of DDTC and DDTC–Ni were obtained using a Fourier transform-far-infrared spectrometer (FT-FIR) (Nicolet 460, Thermo Fisher, USA) with a wavenumber range of 250–500 cm^{-1}. Elemental analysis of the precipitates was conducted using an elemental analyser (Various MACRO, Elementar, Germany).

Thermogravimetric (STA449-F5, NETASCH, Germany) and mass spectrum analysers (QMS 403C, NETZSCH, Germany) were used to analyse the stages of mass loss during the calcination of DDTC–Ni, which measured the gases released during DDTC–Ni pyrolysis. The microstructure and elemental composition of the calcined samples were analysed using a scanning electron microscope (SEM) equipped with energy-dispersive X-ray spectroscopy (EDS; SU-8020, Hitachi, Japan). The calcined samples were characterised by XRD.

2. Results and discussion

2.1. Screening of organic sulphur-containing precipitants for the removal of Ni(II) from simulated strongly acidic wastewater

Fig. 1a shows the Ni(II) removal performance of DDTC, TMT, and STC in simulated strongly acidic wastewater. At DDTC, TMT, and STC dosages of 1.0 g/L, removal efficiencies of approximately 62.0%, 2.4%, and 2.9% were achieved after 20 min, respectively. Using the same precipitants, Zn(II) and Fe(II) removal efficiencies of < 3.0% were achieved. These results demonstrate that, amongst these three precipitants, DDTC could selectively remove nickel ions under strongly acidic conditions.

TMT and STC are widely used to precipitate Ni(II) from weakly acidic, neutral, and weakly alkaline wastewater (Andreottola et al., 2007; Thomas et al., 2018b). However, under strongly acidic conditions, TMT and STC exhibited very low Ni(II)-removal efficiencies. The reaction products were further identified to investigate the underlying mechanism.

A yellow precipitate instantly formed when TMT was added to the wastewater with a sulphuric acid concentration of 1.02 mol/L (Appendix A **Fig. S6**). Furthermore, the FT-IR spectra of TMT (Fig. 1b) exhibited a broad peak near 3383 cm^{-1}, which was attributed to bound water. The peaks at 719 and 1640 cm^{-1} were identified as the C–N [ν(C–N)] and C = N [ν(C = N)] stretching vibrations, respectively (Henke et al., 2001; Guo et al., 2017). Three peaks at 1489, 1240, and 874 cm^{-1} were attributed to the aromatic trithiol in the TMT molecules (Henke et al., 2001). In the FT-IR spectrum of the yellow solid produced, the peaks at 3135, 3040, and 2911 cm^{-1} were attributed to N–H stretching vibration [ν(N–H)]; the 1540, 1125, and 745 cm^{-1} bands were characteristic of the non-aromatic trithione in the TMT molecules; the 1366 cm^{-1} band was attributed to the TMT ring-stretching vibration [νR]; and the 1296 and 1258 cm^{-1} bands were attributed to the symmetric modes of C = S stretching vibration [ν(C = S)] and [νR], respectively (Henke et al., 2001; Cecconi et al., 2003; Liao et al.,
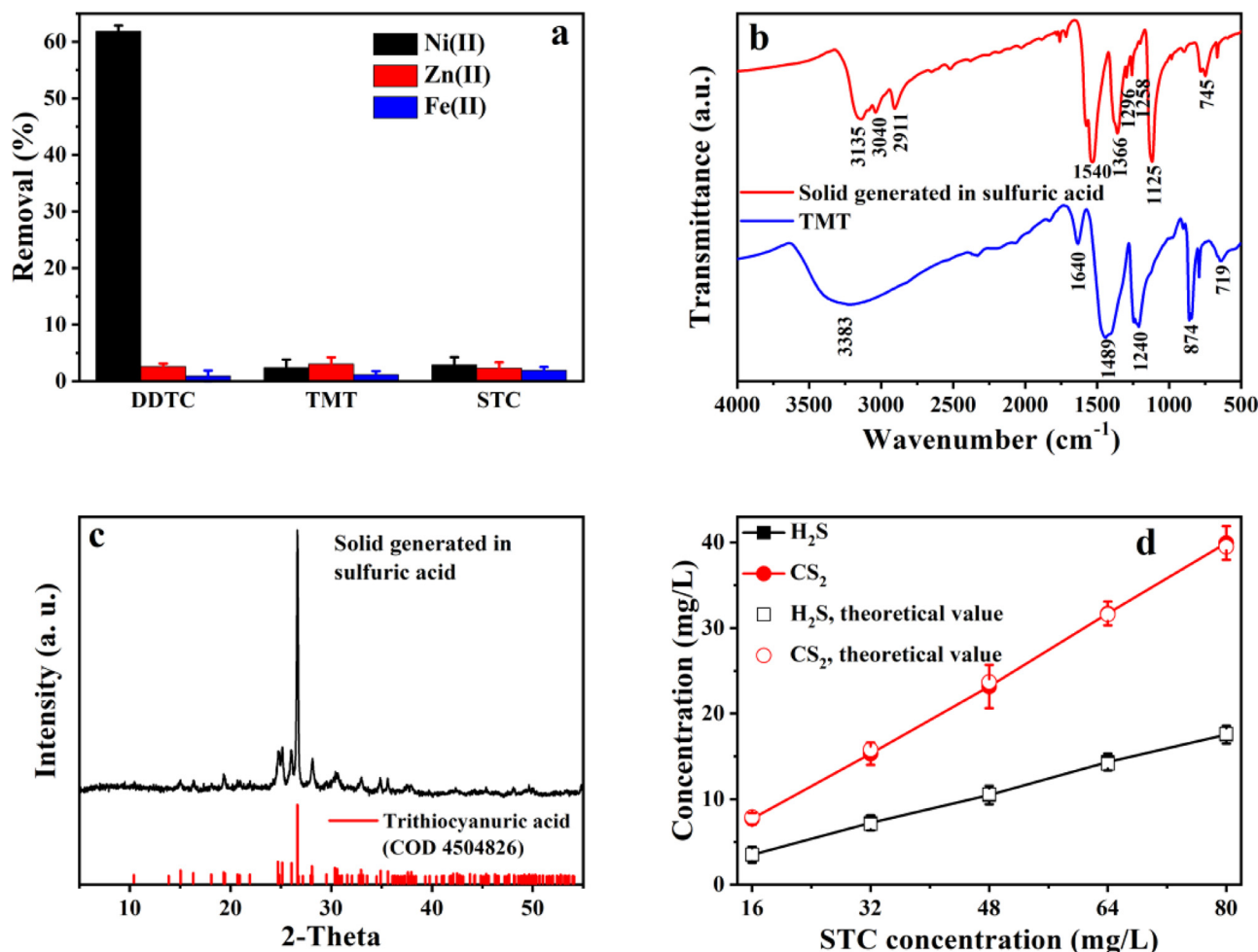
Fig. 1 – (a) The removal efficiency of Ni(II) by DDTC, TMT and STC from strongly acidic wastewater. (b) FT-IR spectra of TMT and its corresponding precipitate. (c) The XRD spectrum of the precipitates generated by TMT precipitation. (d) Concentration of H$_2$S and CS$_2$ generated as a function of STC concentration after 20 min reaction. Conditions: (a) V = 400 mL, Ni(II) 100.0 mg/L, Zn(II) 100.0 mg/L, Fe(II) 300.0 mg/L, H$_2$SO$_4$ 1.02 mol/L, DDTC dosage 1.0 g/L, TMT dosage 1.0 g/L and STC dosage 1.0 g/L; (b) and (c) V 400 mL, H$_2$SO$_4$= 1.02 mol/L and TMT dosage 1.0 g/L; (d) V 400 mL, H$_2$SO$_4$ 1.02 mol/L and STC dosage 1.0 g/L. The error bars showed the standard deviation (n = 3).

2006; Osaka et al., 2009). After comparing the FT-IR spectra of the precipitate and TMT, the characteristic absorption peaks of C = N and aromatic trithiol were not present, while N–H and C = S absorption peaks emerged. These results indicate that aromatic trithiol was transformed into non-aromatic trithione.

The elemental analysis of the precipitate indicated that the mass percentages of C, H, N, and S were 20.33%, 1.80%, 23.77%, and 54.84%, respectively. Therefore, the molar ratio of C:H:N:S in the yellow precipitate was 1:1:1:1, likely indicating the presence of C$_3$H$_3$N$_3$S$_3$. The XRD patterns (Fig. 1c) of the yellow precipitate exhibited a sharp diffraction peak at 2θ = 26.63°, which was consistent with the peak positions for trithiocyanuric acid (H$_3$TMT; COD 4504826). By combining the XRD results and FT-IR spectrum analysis, it can be concluded that TMT transforms into H$_3$TMT in strongly acidic wastewater (Reaction (1)), which is weakly

water-soluble; therefore, its nickel removal efficiency was very low.

$$
\text{(structure)} \quad + 3\text{H}^+ \longrightarrow \text{(structure)} \tag{1}
$$
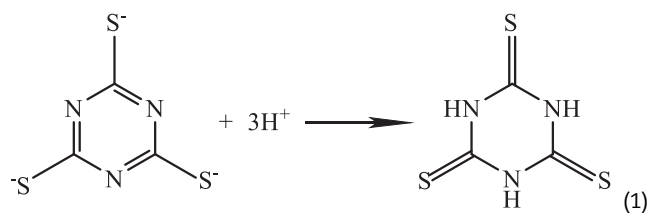
When STC was added to the strongly acidic wastewater, odorous gas was produced that turned wet lead acetate paper black, indicating that the gaseous product was H$_2$S. Therefore, we speculated that CS$_3^{2-}$ can react with H$^+$ to generate H$_2$S and CS$_2$. To verify this, STC was added to the wastewater at a concentration of 1.02 mol/L H$_2$SO$_4$, and the H$_2$S and CS$_2$ con-

centrations were subsequently analysed. Fig. 1d shows that the concentrations of H_2S and CS_2 increased linearly with an increase in the initial STC concentration. Importantly, the H_2S and CS_2 concentrations were consistent with Reaction (2), suggesting that the STC decomposed, rather than precipitated with nickel:

$$CS_3^{2-} + 2H^+ \rightarrow H_2S \uparrow + CS_2 \qquad (2)$$

TMT and STC were generally inefficient in removing Ni(II) from wastewater because, under strongly acidic conditions, TMT transformed into H_3TMT precipitates, while STC decomposed into H_2S and CS_2. Of these three precipitants, DDTC can be used as a potential precipitant under strongly acidic conditions.

2.2. Optimisation of Ni(II)-removal from strongly acidic wastewater using DDTC

To determine the optimal conditions for Ni(II) removal using DDTC, the effects of the DDTC:Ni(II) molar ratio, reaction temperature, reaction time, and H_2SO_4 concentration on the removal efficiency were studied. As the DDTC:Ni(II) molar ratio increased from 1:1 to 3:1, the Ni(II) removal efficiency increased from 30.2% to 80.5%. When the DDTC:Ni(II) molar ratio was further increased to 4:1, a removal efficiency of 99.3% was achieved and maintained thereafter (Fig. 2a). The theoretical optimal molar ratio of DDTC to Ni(II) under neutral conditions is 2:1 (Yan et al., 2016); however, according to our results, the Ni(II)-removal efficiency was only 58.7% at a DDTC:Ni(II) molar ratio of 2:1 under strongly acidic conditions. This indicates that strongly acidic conditions negatively impact the reaction between DDTC and Ni(II).

Previous studies reported that DDTC can decompose into CS_2 and DMA (Reaction (3)) (Miller and Latimer, 1962); therefore, the concentrations of DDTC, CS_2, and DMA after the reaction (Appendix A Fig. S7) were determined. DDTC was not detected after the reactions under the tested molar ratios; however, the concentrations of CS_2 and DMA increased with an increase in the DDTC:Ni(II) molar ratio. Therefore, a portion of the DDTC may react with Ni(II) at a theoretical molar ratio of 2:1 under strongly acidic conditions, while the remainder decomposes to form CS_2 and DMA. We found that the residual concentrations of CS_2 and DMA agreed well with this finding under the employed DDTC:Ni(II) ratios. For example, the residual CS_2 and DMA concentrations were 263.9 and 169.1 mg/L, respectively, at a DDTC:Ni(II) ratio of 4, which are comparable to the corresponding theoretical values of 259.5 and 153.6 mg/L. Therefore, DDTC efficiently removed Ni(II) at a DDTC:Ni(II) molar ratio of 4; at a molar ratio of 2:1, part of the DDTC reacted with Ni(II), and the remainder decomposed into CS_2 and DMA.
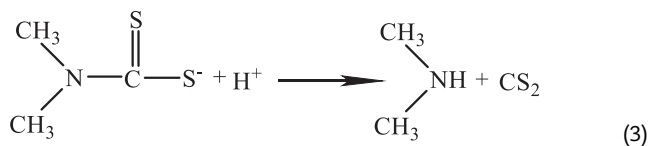
It is necessary to remove the DMA and CS_2 generated during the decomposition of DDTC in the wastewater to prevent secondary pollution. In this study, 30–60-mesh active carbon (1.0 g/L) was used to remove residual CS_2 from the wastewater, and residual DMA was removed using a cation exchange resin (5.0 g/L). Following the treatment process, the residual concentrations of CS_2 and DMA were reduced to 1.1 and 9.3 mg/L, respectively (Appendix A Figs. S8 and S9).

At each DDTC:Ni(II) molar ratio, the Ni(II)-removal efficiency increased rapidly within the first 5 min of the reaction, and tended to stabilise after 10 min. At a DDTC:Ni(II) molar ratio of 4:1, a high Ni(II)-removal efficiency of 99.3% was achieved (Fig. 2b). Therefore, in the following experiments, a DDTC:Ni(II) molar ratio of 4:1 was used and the reaction time was 10 min, unless otherwise stated. An approximate removal efficiency of 99.3% was maintained within the H_2SO_4 concentration range of 0.51–1.02 mol/L. As the H_2SO_4 concentration further increased to 2.55 mol/L, the removal efficiency rapidly decreased to approximately 66.4% (Fig. 2c), indicating that DDTC is suitable for Ni(II) removal at lower H_2SO_4 concentrations.

Within the temperature range of 15–25 °C, the Ni(II)-removal efficiency exceeded 99.0%. As the temperature further increased, the removal efficiency decreased, reaching approximately 2.9% at 40 °C (Fig. 2d). Higher temperatures are conducive to the removal of Ni(II) using dithiocarbamate compounds in the range of 10–60 °C at pH 6.0 (Chen et al., 2018), which contrasts with our findings under strongly acidic conditions. The above results demonstrate that dithiocarbamate compounds can be decomposed into CS_2 and DMA under strongly acidic conditions (Reaction (3)); therefore, it is reasonable to assume that temperature promotes the decomposition of DDTC in strongly acidic wastewater, consequently decreasing the removal efficiency.

Pseudo-first-order and pseudo-second-order kinetic models were employed to understand the DDTC decomposition mechanism. Our results demonstrated that the pseudo-first-order kinetic equation provided the best fitting model ($R^2 > 0.99$) for the DDTC decomposition reaction under strongly acidic conditions (Appendix A Fig. S10). In the temperature range of 15–40 °C, the decomposition rate sharply increased from 1.42 to 8.12 min^{-1} (Appendix A Table S3). Therefore, the low Ni(II)-removal efficiencies observed at high temperatures can be attributed to the decomposition of DDTC.

2.3. Ni(II)-removal mechanisms of DDTC under strongly acidic conditions

The FT-MIR spectra of DDTC and DDTC–Ni are presented in Fig. 3a, and the characteristic peak wavenumbers of functional groups are summarised in Table 1. The characteristic absorption peaks of the S–H group (2711 and 1624 cm^{-1}) that were present in the DDTC spectrum were not present in the DDTC–Ni spectrum, suggesting that this functional group chelated Ni(II). Furthermore, the C = S stretching vibration [ν(C = S)] in the N–C = S functional group of DDTC (1232 cm^{-1}) shifted (to 1238 cm^{-1}) in the DDTC–Ni spectrum, indicating the coordination of Ni(II) with S. The characteristic peaks of [ν(C–S)] (951 cm^{-1}) and [ν(N–CS$_2$)] (1487 cm^{-1}) also shifted to
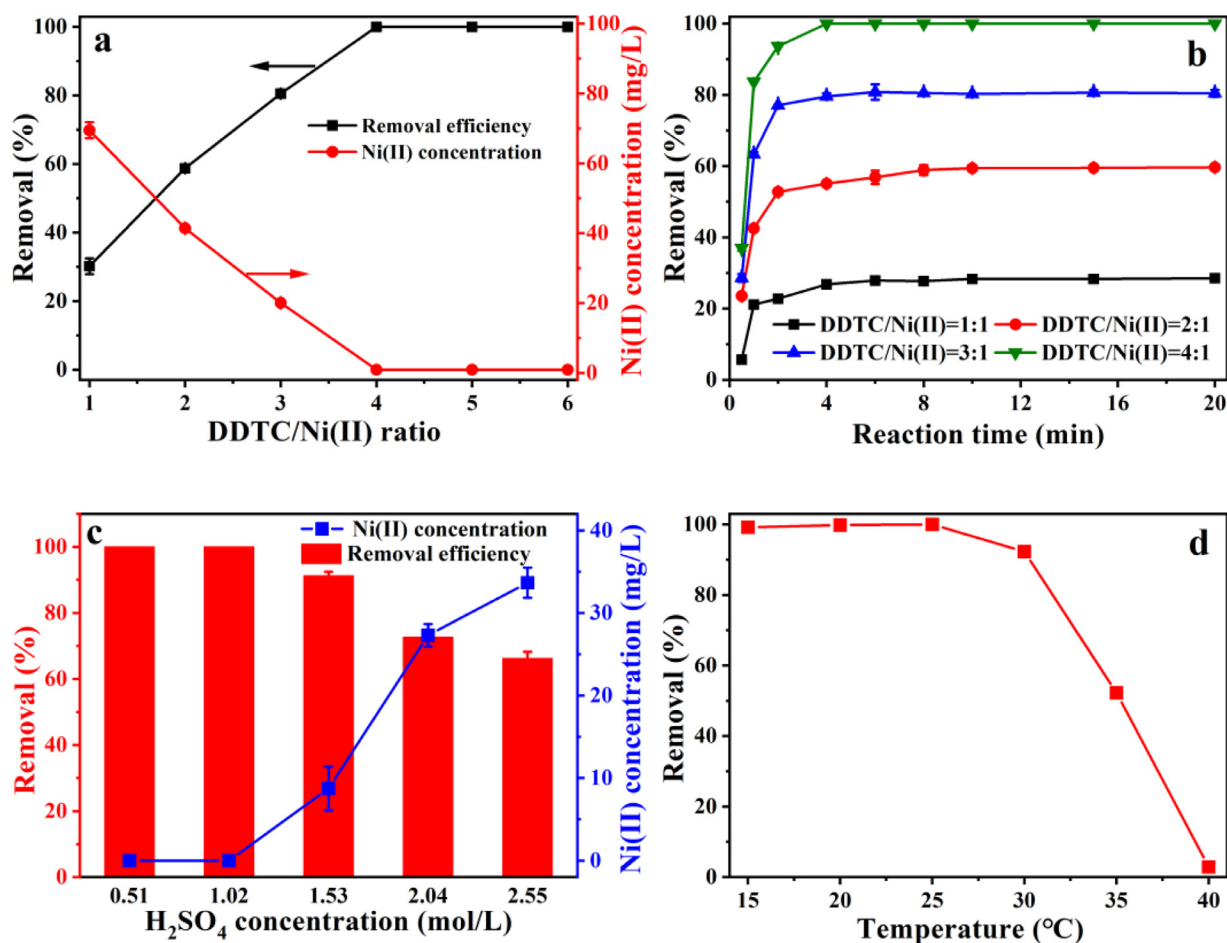
(3)

Fig. 2 – The efficiency of Ni(II) removal from strongly acidic wastewater using DDTC. (a) The removal efficiency as a function of DDTC/Ni(II) ratio. (b) The removal efficiency of Ni(II) as a function of time. (c) The removal efficiency of Ni(II) as a function of H$_2$SO$_4$ concentration. (d) The removal efficiency of Ni(II) as a function of temperature. Conditions: (a) and (b) V 400 mL, Ni(II) 100.0 mg/L, H$_2$SO$_4$ 1.02 mol/L, time 10 min and temperature 25 °C; (c) V 400 mL, Ni(II) 100.0 mg/L, DDTC/Ni(II) 4:1, time 10 min and emperature = 25 °C; (d) V 400 mL, Ni(II) 100.0 mg/L, DDTC/Ni(II) 4:1, H$_2$SO$_4$ 1.02 mol/L and time 10 min. The error bars showed the standard deviation (n = 3).
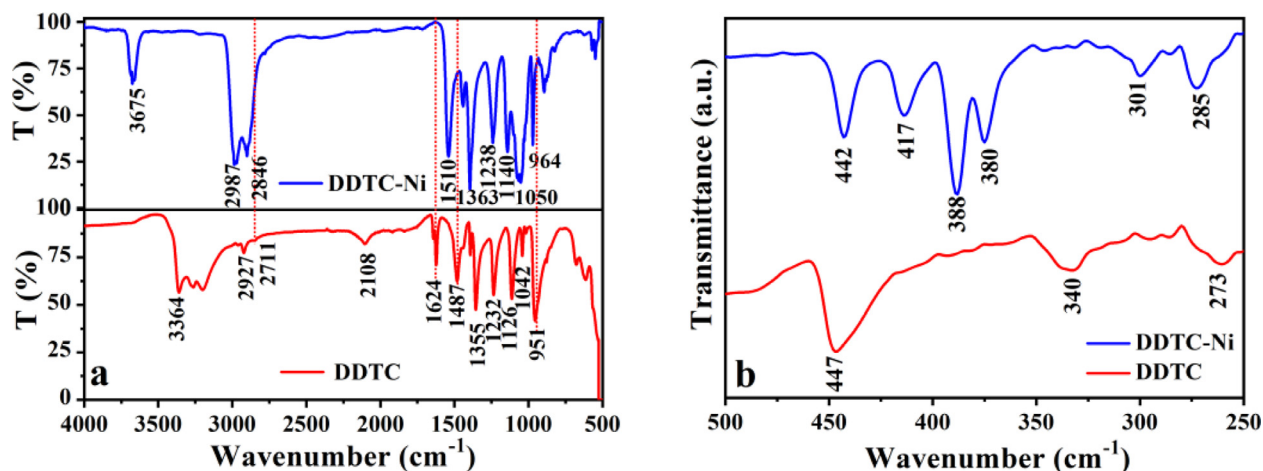

Fig. 3 – FT-IR spectra of DDTC and its corresponding precipitate. (a) FT-MIR spectra. (b) FT-FIR spectra.

Table 1 – The bands and assignments for the vibrational spectra of DDTC and DDTC–Ni.

Group	Absorption peaks (cm^{-1})		References
	DDTC	DDTC–Ni	
Bound water	3364	—	(Xiao et al., 2016)
Adsorbed water	—	3675	(Zhen et al., 2012)
C-H	2927	2987, 2846	(Zhen et al., 2012; Xiao et al., 2016)
S–H	2711, 1624	—	(Zhen et al., 2012)
$C = S$	2108, 1355, 1232, 1126, 1042	1363, 1238, 1140, 1050	(Zhen et al., 2012; Xiao et al., 2016)
N-CS$_2$	1487	1510	(Yan et al., 2016)
C-S	951	964	(Yan et al., 2016)

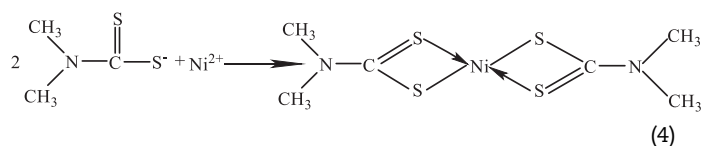**Table 2 – The bands and assignments for the far IR spectra of DDTC and DDTC–Ni.**

Assignment	Bands (cm^{-1})		References
	DDTC	DDTC–Ni	
ω(CNC)	273	—	(Frigerio et al., 1989)
δ(S = C–N), δ(SCS)	340	—	(Nakamoto et al., 1963; Frigerio et al., 1989)
δ(CNC)	447	442, 417	(Kellner and St. Nikolov, 1981; Frigerio et al., 1989)
ρ(CNC)	—	388	(Kellner and St. Nikolov, 1981)
νs(NiS)	—	380	(Kellner and St. Nikolov, 1981; Payne et al., 1985)
δ_s(CSNi)	—	301	(Alexiev, 1995)
δas(SNiS)	—	285	(Kellner and St. Nikolov, 1981)

964 and 1510 cm^{-1}, respectively, demonstrating that the band energy of these bonds was increased. During the reaction between DDTC and Ni(II), a coordination bond forms between the S atoms of DDTC and Ni(II) due to the large radius, negative charge, and spontaneous polarisation of S atoms in DDTC (Bai et al., 2011; Zhen et al., 2012; Ayalew et al., 2020). Furthermore, the coordination of S atoms with Ni(II) shortened the length of the N–C bonds, thereby increasing the band energy of N–C bonds, which is indicated as the blue shift of N–CS$_2$ bonds in the infrared spectra (Xiao et al., 2016). The blue shift of C–S bonds in the DDTC indicates the presence of partial double bonds in the C–S groups after the chelation of DDTC and Ni(II) (Xiao et al., 2016). Overall, the observed FT-MIR spectral differences confirm that the precipitation between DDTC and Ni(II) was facilitated by the formation of coordination bonds between S atoms and Ni(II).

The FT-FIR spectra of DDTC and DDTC–Ni are illustrated in Fig. 3b, and the bands and assignments for the spectra are summarised in Table 2. In the DDTC–Ni FT-FIR spectrum, the bands at 380, 301, and 285 cm^{-1} were attributed to ν_s(NiS), δ_s(CSNi), and δ_{as}(SNiS), respectively. These signals all indicate that, during the reaction between DDTC and Ni(II), a stronger sulphur-nickel bond formed between Ni(II) and the dithiocarbamate groups.

Elemental analysis revealed that the mass percentages of C, H, N, and S in the DDTC—Ni were 24.24%, 4.08%, 9.64%, and 41.47%, respectively. Therefore, the molar ratio of C:H:N:S in the DDTC–Ni was 3:6:1:2, and the likely chemical formula was

C$_6$H$_{12}$N$_2$S$_4$Ni. Based on the FT-IR spectral analysis, the reaction between DDTC and Ni(II) could be described by (Reaction (4)):

$$2 \quad \underset{CH_3}{\overset{CH_3}{N}}-C\overset{S}{\underset{}{\parallel}}-S^- + Ni^{2+} \longrightarrow \underset{CH_3}{\overset{CH_3}{N}}-C\overset{S}{\underset{S}{<}}Ni\overset{S}{\underset{S}{>}}C-N\overset{CH_3}{\underset{CH_3}{<}}$$

(4)

2.4. Recovery of nickel oxide by the calcination of DDTC–Ni

After the reaction between DDTC and Ni(II), 1.0-g precipitate (DDTC–Ni) samples were obtained from 2-L samples of the simulated wastewater. Nickel flash smelting furnaces are widely used in the nickel smelting industry. Therefore, we aimed to recover NiO from DDTC–Ni by thermal decomposition. As shown in Fig. 4a, the pronounced XRD peaks of 37.20°, 43.10°, 62.80°, 75.41°, and 79.50° at 2θ corresponded to the (111), (200), (220), (311), and (222) lattices of crystalline NiO, respectively, which agreed with the standard data (JCPDS 04–0835) (Al-Sehemi et al., 2014). The sharp peaks imply that the thermal treatment produced a well-crystallised nickel oxide structure. Based on the XRD peaks, the average crystallite particle size of NiO was 63.1 nm, as calculated using the Scherrer for-
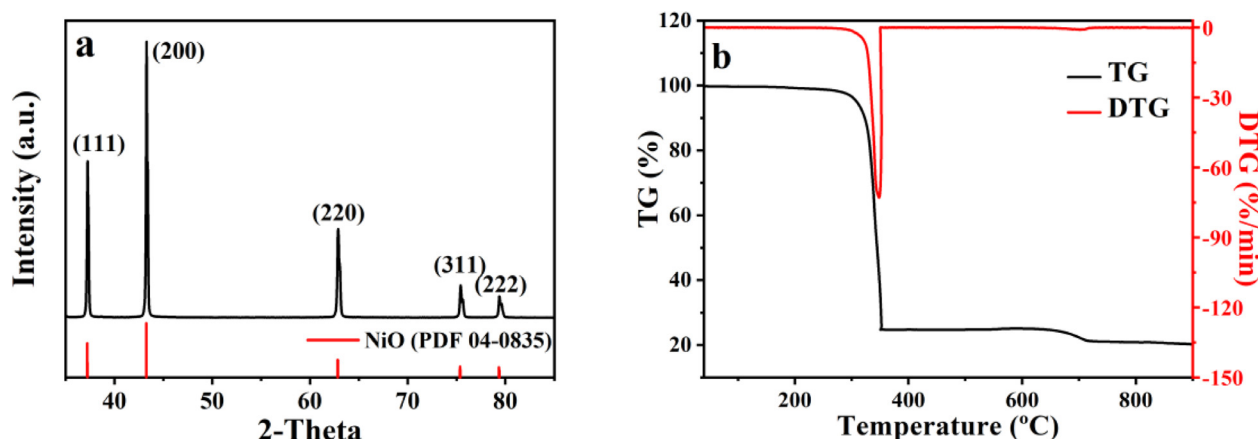
Fig. 4 – (a) X-ray diffraction patterns of NiO obtained. (b) TG/DTG curves of DDTC–Ni.

mula (Yu et al., 2013):

$$D = \frac{0.9\lambda}{\beta \cos \theta} \tag{5}$$

where D is the crystallite particle size, λ is the x-ray wavelength, β is the full width at half the maximum intensity of the peak position, and θ is the diffraction angle.

The calcined product was visualised using SEM (Appendix A **Fig. S11**), which indicated that the particles were nanosized and uniform, and most were irregularly dispersed microspheres. The EDS spectra of the calcined product (Appendix A **Fig. S12**) show that Ni and O were the only elements in the product, further suggesting that the product was NiO. The atomic percentages of Ni and O were 49.54% and 50.46%, respectively, indicating that high-purity NiO was obtained. In our experiments, 0.25 g of NiO was obtained from 2 L of simulated strongly acidic wastewater containing 98.9 mg/L of Ni(II) and 1.02 mol/L H_2SO_4, and the recovery efficiency reached 98.2%.

The TG/DTG graph (Fig. 4b) shows that DDTC–Ni lost its weight in two stages, with a 72.3% mass loss in the first stage within the temperature range of 248–372 °C and an endothermic peak at 349 °C. In the second stage, the mass loss was approximately 3.2%, which began at approximately 522 °C, and led to the formation of stable phases at approximately 760 °C. The residual DDTC–Ni mass was 24.5%. The evolution of ion-fragments released by different gaseous products of DDTC–Ni calcination is shown in Fig. 5 as the relationship between the ion current and temperature. The thermal decomposition of DDTC–Ni was continuous, and SO_2, CO_2, H_2O, NO_2, and CS_2 were released. Previous studies on the thermal behaviour of metal-dithiocarbamates in air indicated that the decomposition of metal-dithiocarbamates usually follows these steps (Sharma, 1986; Cavalheiro et al., 2000):
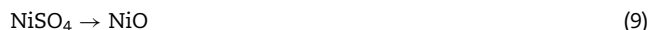
Decomposition of dithiocarbamate to thiocyanate:

$$Ni(C_3H_6NS_2)_2 \rightarrow Ni(CNS)_2 \tag{6}$$

Decomposition of thiocyanate to sulphide:

$$Ni(CNS)_2 \rightarrow NiS \tag{7}$$

Oxidation of sulphide to metal oxide:

$$NiS \rightarrow NiO + NiSO_4 \tag{8}$$

$$NiSO_4 \rightarrow NiO \tag{9}$$

The release of SO_2 during thermal treatment occurred in three distinct stages with peaks at 351, 524, and 759 °C, which were associated with nickel dithiocarbamate decomposition into nickel thiocyanate, nickel thiocyanate decomposition into nickel sulphide, and nickel sulphide oxidation into nickel oxide, respectively, according to the SO_2 ion current curve. The release of CO_2 from DDTC–Ni occurred across a wide temperature range (298–760 °C). The low-temperature peak at approximately 350 °C reflected the decomposition of nickel dithiocarbamate to nickel thiocyanate. A small amount of CO_2 was produced during the decomposition of nickel thiocyanate above 470 °C. According to the H_2O ion current curve, H_2O released in the range of 325–409 °C, with a peak at 348 °C. The release of H_2O was attributed to the decomposition of nickel dithiocarbamate to nickel thiocyanate. Within the temperature range of 320–390 °C, CS_2 evolution occurred and the CS_2 ion current curve peaked at 346 and 370 °C, respectively. The release of CS_2 was attributed to the decomposition of nickel dithiocarbamate into nickel thiocyanate. NO_2 was released in the temperature range of 328–436 °C, with the peaks at approximately 346 and 364 °C reflecting the decomposition of nickel dithiocarbamate into nickel thiocyanate. At higher temperatures (> 436 °C), trace amounts of NO_2 were generated through the decomposition of nickel thiocyanate.

Based on these observations, the gaseous products generated during the first stage of DDTC–Ni mass loss (i.e., at 248−372 °C) included NO_2, CS_2, SO_2, CO_2, and H_2O, and the second stage of mass loss (i.e., at 522−760 °C) involved the generation of SO_2 and CO_2. CS_2 may oxidise to SO_2, CO_2, and CO under high-temperature conditions (600–800 °C) (Zeng et al., 2019). Nickel smelting is also a source of gaseous emissions, including SO_2, CO_2, CO, and NO_x, which is consistent with the release of gases from the recovery of NiO from DDTC–Ni. Therefore, the gas pollutants generated during the DDTC–Ni
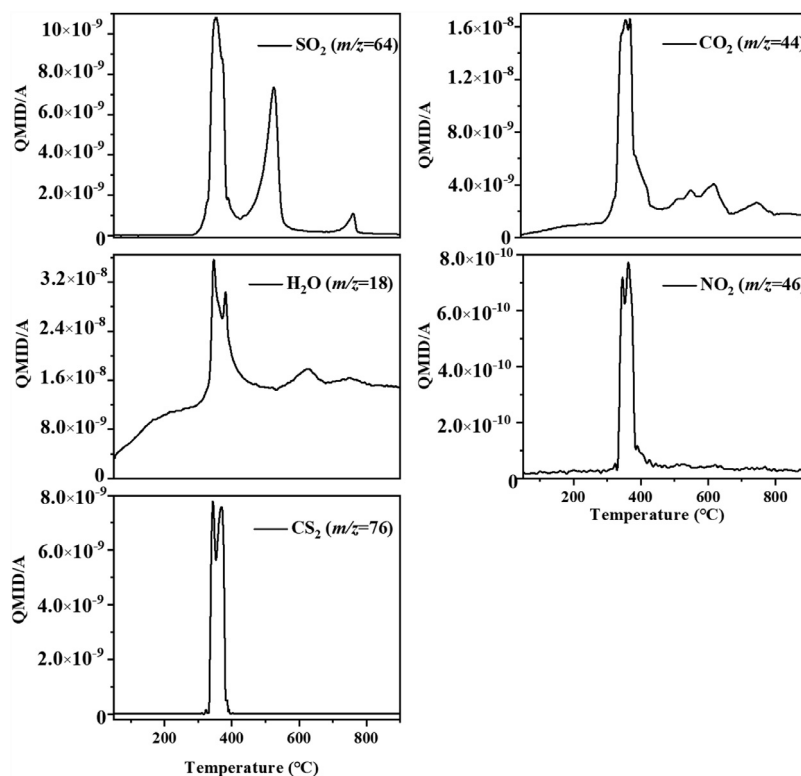
Fig. 5 – Evolved gas analysis during DDTC–Ni calcination.

calcination process can be treated using the same equipment employed in the treatment of nickel smelter emissions.

2.5. *Nickel recovery from industrial wastewater*

To verify the practical application of Ni(II) recovery using DDTC, experiments were conducted using wastewater from an industrial smelter (Appendix A **Fig. S13**). These experiments indicated that, at a DDTC:Ni(II) molar ratio of 4, approximately 99.5% of the Ni(II) was removed after 10 min, with a residual Ni(II) concentration of 0.5 mg/L (Fig. 6). Some of the DDTC decomposed in these reactions, resulting in residual DMA and CS_2 in the treated wastewater. These residual substances could be removed using active carbon (1.0 g/L) and cation exchange resin (5.0 g/L), with residual CS_2 and DMA concentrations of 0.9 and 8.3 mg/L, respectively. The recovered precipitates were calcined to recover nickel oxide (Appendix A **Fig. S14**), achieving a high Ni-recovery efficiency of 95.3%.

To reflect the industrial application potential of this process, we estimated the economic benefits of this process in recovering nickel from strongly acidic wastewater. On the basis of existing production equipment, a chelating precipitation-calcination process was developed to remove Ni(II) from strongly acidic wastewater, and recover NiO from the precipitate. There is no need to add additional equipment besides the cost of chemicals. The treatment cost of strongly acidic nickel-containing wastewater can be estimated by the price of DDTC, considering that activated carbon and cation exchange resin can be reused. According to the market price of China in 2020, the cost of industrial DDTC is approximately $1142.4 per ton.
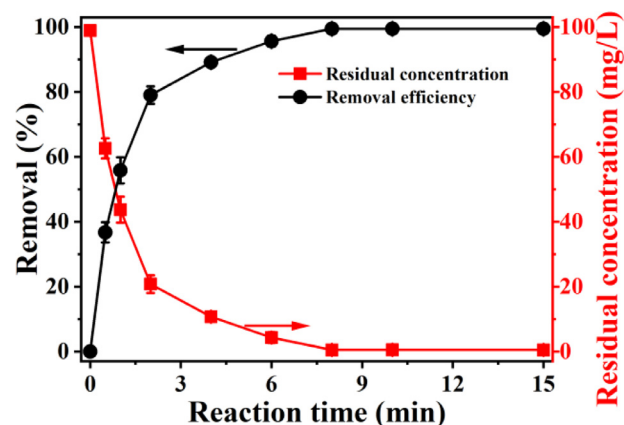

Fig. 6 – Removal of Ni(II) by DDTC from real wastewater. Conditions: V 5 L, DDTC/Ni(II) 4:1, Ni(II) 98.9 mg/L, room temperature. The error bars showed the standard deviation (n = 3).

For the actual wastewater containing 98.9 mg/L Ni(II), 0.8 M H_2SO_4, and other cations (Appendix A **Table S1**) collected from the nickel smelter, the required DDTC dosage is 1.2 kg/m^3, and the cost is calculated to be $1.4 per m^3. Additionally, 120.6 g of NiO can be recovered per cubic metre of wastewater treated. The current market price for industrial NiO is approximately $34,000 per ton, and the price of recovered NiO is calculated to be $4.1 per m^3. Therefore, taking the actual acidic wastewater containing 98.9 mg/L Ni(II) as an example, the economic ben-

efit of the proposed method is estimated to be \$2.7 per m^3. Above all, the proposed method has achieved high recovery efficiency of nickel from strongly acidic wastewater and produced immeasurable economic benefits.

3. Conclusions

An organic sulphur-containing precipitant, DDTC, was evaluated alongside TMT and STC for removing Ni(II) from strongly acidic wastewater. At a DDTC:Ni(II) molar ratio of 4:1 and temperature of 25 °C, a Ni(II)-removal efficiency of 99.3% was achieved after 10 min of reaction in strongly acidic wastewater with 1.02 mol/L H$_2$SO$_4$. Under these conditions, coordination bonds formed between the Ni(II) and S atom of the dithiocarbamate groups of DDTC, and DDTC–Ni was precipitated at a DDTC:Ni(II) molar ratio of 2:1. The remaining DDTC decomposed into CS$_2$ and DMA. Importantly, high-purity NiO was successfully recovered via the calcination of the DDTC–Ni precipitates, with recovery efficiencies of up to 98.2%. The gases released during the calcination process were identified as NO$_2$, CS$_2$, H$_2$O, CO$_2$, and SO$_2$. These results provide a basis for the effective recovery of Ni(II) from strongly acidic wastewater.

Acknowledgments

Appendix A Supplementary data

Supplementary material associated with this article can be found, in the online version, at doi:10.1016/j.jes.2020.12.014.

REFERENCES

Al-Sehemi, A.G., Al-Shihri, A.S., Kalam, A., Du, G.H., Ahmad, T., 2014. Microwave synthesis, optical properties and surface area studies of NiO nanoparticles. J. Mol. Struct. 1058, 56–61.

Andreottola, G., Cadonna, M., Foladori, P., Gatti, G., Lorenzi, F., Nardelli, P., 2007. Heavy metal removal from winery wastewater in the case of restrictive discharge regulation. Water Sci. Technol. 56 (2), 111–120.

Ayalew, Z.M., Zhang, X.Y., Guo, X.J., Ullah, S., Leng, S.W., Luo, X.Y., et al., 2020. Removal of Cu, Ni and Zn directly from acidic electroplating wastewater by Oligo-Ethyleneamine dithiocarbamate (OEDTC). Sep. Purif. Technol. 248, 117114.

Bai, L., Hu, H.P., Fu, W., Wan, J., Cheng, X.L., Zhuge, L., et al., 2011. Synthesis of a novel silica-supported dithiocarbamate adsorbent and its properties for the removal of heavy metal ions. J. Hazard. Mater. 195, 261–275.

Cavalheiro, É.T.G., Ionashiro, M., Marino, G., Breviglieri, S.T., Chierice, G.O., 2000. Correlation between i.r. spectra and thermal decomposition of cobalt(II), nickel(II), copper(II) and mercury(II) complexes with piperidinedithiocarbamate and pyrrolidinedithiocarbamate. Trans. Met. Chem. 25, 69–72.

Cecconi, F., Ghilardi, C.A., Midollini, S., Orlandini, A., 2003. s-Block metal complexes of 2,4,6-trimercaptotriazine. Synthesis and X-ray characterization of two polymeric [Na(H$_2$O)$_3$(H$_2$TMT)]$_n$ and [K$_3$(H$_2$O)$_6$(H$_2$TMT)$_3$(H$_3$TMT)]$_n$ compounds. Inorg. Chim. Acta 343, 377–382.

Chen, D., Cui, P.L., Cao, H.B., Yang, J., 2015. A 1-dodecanethiol-based phase transfer protocol for the highly efficient extraction of noble metal ions from aqueous phase. J. Environ. Sci. 29 (3), 146–150.

Chen, H., Zhao, Y., Yang, Q., Yan, Q., 2018. Preparation of poly-ammonium/sodium dithiocarbamate for the efficient removal of chelated heavy metal ions from aqueous environments. J. Environ. Chem. Eng. 6, 2344–2354.

Coman, V., Robotin, B., Ilea, P., 2013. Nickel recovery/removal from industrial wastes: a review. Resour. Conserv. Recycl. 73, 229–238.

Decostere, B., Hogie, J., Dejans, P., Van Hulle, S.W.H., 2009. Removal of heavy metals occurring in the washing water of flue gas purification. Chem. Eng. J. 150, 196–203.

Deep, A., Kumar, P., Carvalho, J.M.R., 2010. Recovery of copper from zinc leaching liquor using ACORGA M5640. Sep. Purif. Technol. 76, 21–25.

Frigerio, A., Halac, B., Perec, M., 1989. Spectroscopic characterization of anionic tris(N,N-dialkyldithiocarbamate) complexes of zinc(II) and cadmium(II). Inorg. Chim. Acta 164, 149–154.

Fu, F.L., Chen, R.M., Xiong, Y., 2007. Comparative investigation of N,N'-bis-(dithiocarboxy)piperazine and diethyldithiocarbamate as precipitants for Ni(II) in simulated wastewater. J. Hazard. Mater. 142, 437–442.

Guo, F., Shi, W.L., Guo, S.J., Guan, W.S., Liu, Y.H., Huang, H., et al., 2017. Ni$_3$(C$_3$N$_3$S$_3$)$_2$ coordination polymer as a novel broad spectrum-driven photocatalyst for water splitting into hydrogen. Appl. Catal. B Environ. 210, 205–211.

Henke, K.R., Hutchison, A.R., Krepps, M.K., Parkin, S., Atwood, D.A., 2001. Chemistry of 2,4,6-trimercapto-1,3,5-triazine (TMT): acid dissociation constants and group 2 complexes. Inorg. Chem. 40 (17), 4443–4447.

Hunt, E.C., Mcnally, W.A., Smith, A.F., 1973. A modified field test for the determination of carbon disulphide vapour in air. Analyst 98, 585–592.

Hussain, M.M., Rahman, M.M., Asiri, A.M., 2017. Ultrasensitive and selective 4-aminophenol chemical sensor development based on nickel oxide nanoparticles decorated carbon nanotube nanocomposites for green environment. J. Environ. Sci. 53 (3), 27–38.

Iliev, V., Alexiev, V., 1995. EPR, 1H, 31P ENDOR, and IR study of Cu(II) and Ni(II) (O,O-dimethyldithiophosphate) (N,N-dimethyldithiocarbamate) complexes. Spectrochim. Acta 51A (6), 969–977.

Karbanee, N., Van Hille, R.P., Lewis, A.E., 2008. Controlled nickel sulfide precipitation using gaseous hydrogen sulfide. Ind. Eng. Chem. Res. 47, 1596–1602 2008.

Kellner, R., Nikolov, St., 1981. Far IR spectra of dithiocarbamate complexes correlations with structure parameters. J. Inorg. Nucl. Chem. 43, 1183–1188.

Kong, L.H., Peng, X.J., Hu, X.Y., 2017. Mechanisms of UV-light promoted removal of As(V) by sulfide from strongly acidic wastewater. Environ. Sci. Technol. 51, 12583–12591.

Lewis, A.E., 2010. Review of metal sulphide precipitation. Hydrometallurgy 104, 222–234.

Li, F., Liu, H.Y., Xue, C.H., Xin, X.Q., Xu, J., Chang, Y.G., et al., 2009. Simultaneous determination of dimethylamine, trimethylamine and trimethylamine-n-oxide in aquatic products extracts by ion chromatography with non-suppressed conductivity detection. J. Chromatogr. A 1216, 5924–5926.

Li, L.Q., Zhong, H., Cao, Z.F., Yuan, L., 2011. Recovery of copper(II) and nickel(II) from plating wastewater by solvent extraction. Chin. J. Chem. Eng. 19 (6), 926–930.

Liao, D.M., Luo, Y.B., Yu, P., Chen, Z.G., 2006. Chemistry of copper trimercaptotriazine (TMT) compounds and removal of copper from copper-ammine species by TMT. Appl. Organomet. Chem. 20, 246–253.

Matlock, M.M., Henke, K.R., Atwood, D.A., 2002. Effectiveness of commercial reagents for heavy metal removal from water with new insights for future chelate designs. J. Hazard. Mater. 92, 129–142.

Matlock, M.M., Howerton, B.S., Aelstyn, M.Van., Henke, K.R., Atwood, D.A., 2003. Soft metal preferences of 1,3-benzenediamidoethanethiol. Water Res 37, 579–584.

Miller, D.M., Latimer, R.A., 1962. The kinetics of the decomposition and synthesis of some dithiocarbamates. Can. J. Chem. 40, 246–255.

Nakamoto, K., Fujita, J., Condrate, R.A., Morimoto, Y., 1963. Infrared spectra of metal chelate compounds. IX. A normal coordinate analysis of dithiocarbamato complexes. J. Chem. Phys. 39 (2), 423–427.

Orhan, G., Arslan, C., Bombach, H., Stelter, M., 2002. Nickel recovery from the rinse waters of plating baths. Hydrometallurgy 65, 1–8.

Osaka, N., Ishitsuka, M., Hiaki, T., 2009. Infrared reflection absorption spectroscopic study of adsorption structure of self-assembled monolayer film of trithiocyanuric acid on evaporated silver film. J. Mol. Struct. 921, 144–149.

Payne, R., Magee, R.J., Liesegang, J., 1985. (II) Infrared and X-ray photoelectron spectroscopy of some transition metal dithiocarbamates and xanthate. J. Electron. Spectrosc. 35, 113–130.

Pearson, R.G., 1968. Hard and soft acids and bases, HSAB, part I: fundamental principles. J. Chem. Educ. 45 (9), 581–587.

Peng, C.S., Jin, R.J., Li, G.Y., Li, F.S., Gu, Q.B., 2014. Recovery of nickel and water from wastewater with electrochemical combination process. Sep. Purif. Technol. 136, 42–49.

Sharma, A.K., 1986. Thermal behaviour of metal-dithiocarbamates. Thermochim. Acta 104, 339–372.

Silva, M.S.P, Da Silva, I.S., Abate, G., Masini, J.C., 2001. Spectrophotometric determination of acid volatile sulfide in river sediments by sequential injection analysis exploiting the methylene blue reaction. Talanta 53, 843–850.

Sulaiman, R.N.R., Othman, N., 2018. Solvent extraction of nickel ions from electroless nickel plating wastewater using synergistic green binary mixture of D2EHPA-octanol system. J. Environ. Chem. Eng. 6, 1814–1820.

Tanaka, M., Huang, Y., Yahagi, T., Hossain, M.K., Sato, Y., Narita, H., 2008. Solvent extraction recovery of nickel from spent electroless nickel plating baths by a mixer-settler extractor. Sep. Purif. Technol. 62, 97–102.

Tao, X.W., Liu, F.Q., Bai, Z.Q., Wei, D.Y., Zhang, X.P., Wang, J.F., et al., 2016. Insight into selective removal of copper from high-concentration nickel solutions with XPS and DFT: new technique to prepare 5N-nickel with chelating resin. J. Environ. Sci. 48 (10), 34–44.

Thomas, M., Zdebik, D., Białecka, B., 2018a. Using sodium trithiocarbonate to precipitate heavy metals from industrial wastewater – from the laboratory to industrial scale. Polish J. Environ. Stud. 27 (4), 1753–1763.

Thomas, M., Zdebik, D., Białecka, B., 2018b. Use of sodium trithiocarbonate for remove of chelated copper ions from industrial wastewater originating from the electroless copper plating process. Arch. Environ. Prot. 44 (2), 32–42.

Vandebeek, R.R., Joris, S.J., Aspila, K.I., Chakrabarti, C.L., 1970. Decomposition of some cyclic dithiocarbamates. Can. J. Chem. 48, 2204–2209.

Wei, Q.F., Ren, X.L., Guo, J.J., Chen, Y.X., 2016. Recovery and separation of sulfuric acid and iron from dilute acidic sulfate effluent and waste sulfuric acid by solvent extraction and stripping. J. Hazard. Mater. 304, 1–9.

Xiao, X., Ye, M.Y., Yan, P.F., Qiu, Y.Q., Sun, S.Y., Ren, J., et al., 2016. Disodium N,N-bis-(dithiocarboxy)ethanediamine: synthesis, performance, and mechanism of action toward trace ethylenediaminetetraacetic acid copper(II). Environ. Sci. Pollut. Res. 23, 19696–19706.

Yan, P.F., Ye, M.Y., Sun, S.Y., Xiao, X., Dai, W.C., Zhang, N., 2016. Removal performances and mechanisms of action towards ethylenediaminetetraacetic acid nickel(II) salt by dithiocarbamate compounds having different carbon chain lengths. J. Clean. Prod. 122, 308–314.

Yan, P.F., Ye, M.Y., Guan, Z.J., Sun, S.Y., Guo, Y.P, Liu, J.Y., 2019. Synthesis of magnetic dithiocarbamate chelating resin and its absorption behavior for ethylenediaminetetraacetic acid copper. Process. Saf. Environ. 123, 130–139.

Yu, L., Peng, X.J., Ni, F., Li, J., Wang, D.S., Luan, Z.K., 2013. Arsenite removal from aqueous solutions by γ-Fe_2O_3-TiO_2 magnetic nanoparticles through simultaneous photocatalytic oxidation and adsorption. J. Hazard. Mater. 246–247, 10–17.

Zeng, Z., Dlugogorski, B.Z., Oluwoye, I., Altarawneh, M., 2019. Combustion chemistry of carbon disulphide (CS_2). Combust. Flame 210, 413–425.

Zhang, X.F., Tian, J., Hu, Y.H., Han, H.S., Luo, X.P., Sun, W., et al., 2020. Selective sulfide precipitation of copper ions from arsenic wastewater using monoclinic pyrrhotite. Sci. Total Environ. 705, 135816.

Zhen, H.B., Xu, Q., Hu, Y.Y., Cheng, J.H., 2012. Characteristics of heavy metals capturing agent dithiocarbamate (DTC) for treatment of ethylene diamine tetraacetic acid-Cu (EDTA-Cu) contaminated wastewater. Chem. Eng. J. 209, 547–557.